

A BICM-IDD Scheme for Non-Coherent MIMO Communication

Mohamed A. El-Azizy, Ramy H. Gohary, and Timothy N. Davidson

Abstract—A bit-interleaved coded modulation (BICM) scheme with iterative (soft) demapping and decoding (IDD) is developed for non-coherent communication over a multiple-input multiple-output (MIMO) channel. The scheme exploits the underlying Grassmannian geometry of the signalling scheme that approaches the ergodic capacity of the non-coherent model at high signal-to-noise ratios. In particular, this geometry guides the construction of the constellation and the mapper at the transmitter, and gives rise to a computationally-efficient list-based demapping algorithm. The incorporation of a scheme that enables the decoder to augment the demapping list virtually eliminates the mild performance degradation of the efficient demapper. Simulation results demonstrate that at high data rates the proposed scheme can provide significantly better performance than several training-based BICM-IDD schemes.

Index Terms—Ergodic capacity, Grassmannian signalling, iterative decoding, list demapping, training, mismatched decoding.

I. INTRODUCTION

IN a standard model for multiple-input multiple-output (MIMO) communication, the receiver is assumed to have complete channel state information (CSI) *a priori*, which enables coherent detection. An alternative framework that accounts for the communication resources that would need to be expended to acquire the CSI is the non-coherent model, in which the receiver does not have any *a priori* CSI; e.g., [1]. Under a standard model for narrow-band communication in a richly-scattered environment, the high signal-to-noise ratio (SNR) ergodic capacity of the non-coherent model is a significant fraction of that of the coherent model. However, the underlying geometry of the corresponding signalling scheme is significantly different [1]–[3]. In particular, the high-SNR capacity achieving channel symbols are unitary matrices that span isotropically distributed linear subspaces [1], [2]. In such a system, the information is conveyed by the subspaces rather than the matrices themselves, and these subspaces can be represented by points on a compact Grassmann manifold [3]. The purpose of this paper is to develop a pragmatic coded Grassmannian transceiver that provides low error rates at data rates close to the ergodic capacity of the non-coherent MIMO channel.

Manuscript received August 10, 2007; revised December 27, 2007 and March 20, 2008; accepted March 20, 2008. The associate editor coordinating the review of this letter and approving it for publication was H. A. Nguyen.

This work was supported in part by Communications and Information Technology, Ontario, a Premier's Research Excellence Award from the Government of Ontario, and by the Natural Sciences and Engineering Research Council of Canada. The work of the third author is also supported in part by the Canada Research Chairs program.

The authors are with the Department of Electrical and Computer Engineering, McMaster University, Hamilton, Ontario, Canada (e-mail: {goharyrh, davidson}@mcmaster.ca).

A preliminary version of a portion of this work appears in *Proc. IEEE Int. Conf. Commun.*, Istanbul, June 2006.

Digital Object Identifier 10.1109/TWC.2009.070887

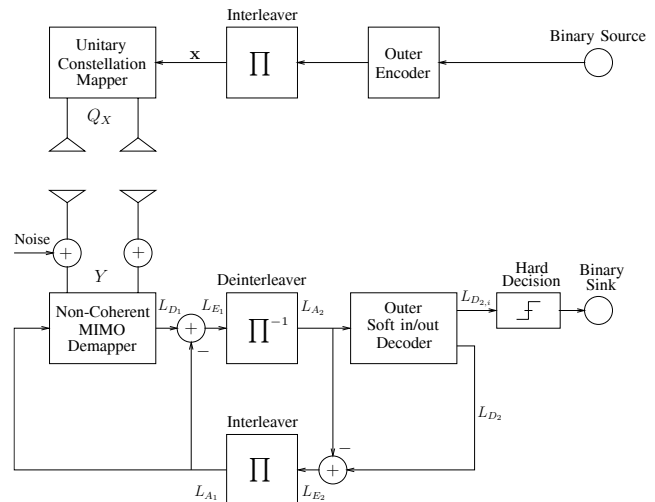


Fig. 1. A BICM-IDD scheme for non-coherent MIMO communication.

The proposed transceiver is based on the principle of bit-interleaved coded modulation (BICM) [4] with iterative (soft) demapping and decoding (IDD), e.g., [5], and is illustrated in Figure 1. Some coded schemes for the non-coherent MIMO channel have previously been proposed (e.g., [6]–[9]), but our scheme directly exploits the underlying Grassmannian geometry of the optimal signalling scheme at high SNRs. This geometry guides the construction of the Grassmannian constellations and the mapper at the transmitter, and gives rise to an efficient list-based demapping algorithm that substantially reduces the computational complexity of the receiver. Furthermore, we suggest a method that enables the decoder to augment the list used by the demapper, and we demonstrate that this feature virtually eliminates the mild performance degradation of the efficient demapper.

An alternative to the Grassmannian signalling approach to high-SNR non-coherent MIMO communication is to transmit a block of training symbols, and then communicate in a coherent mode [10]–[12]. We compare the performance of the proposed scheme to that of two classes of training-based BICM-IDD schemes, one with a “mismatched” demapping metric that presumes that an explicit channel estimate is precise, and another with the “optimum” metric that does not involve explicit channel estimation; cf. [13]. Simulation results show that at high data rates the proposed scheme can provide significantly better performance than these training-based schemes.

II. SYSTEM MODEL

We consider a system with M transmit antennas and N receive antennas communicating over a frequency-flat richly-scattered block-fading channel of coherence time $T \geq$

$\min(M, N) + N$,¹ with $M = \min\{\lfloor T/2 \rfloor, N\}$; cf. [3]. We will denote the signal vector transmitted at each channel use by the rows of a $T \times M$ matrix \mathbf{Q}_X , and hence the $T \times N$ received signal matrix \mathbf{Y} is

$$\mathbf{Y} = \mathbf{Q}_X \mathbf{H} + \mathbf{V}, \quad (1)$$

where \mathbf{H} is the $M \times N$ channel matrix whose entries are drawn independently from the standard complex Gaussian distribution $\mathcal{CN}(0, 1)$, and \mathbf{V} is the $T \times N$ additive noise matrix whose entries are drawn independently from $\mathcal{CN}(0, M/(\rho T))$, where ρ is the signal-to-noise ratio.

In the non-coherent scenario, neither the transmitter nor the receiver knows \mathbf{H} , and the capacity achieving input signals for high-SNR operation are $T \times M$ (tall) unitary matrices that span isotropically distributed subspaces [1], [3]. The columns of each such matrix \mathbf{Q}_X span an M -dimensional subspace that can be represented by a ‘‘constellation’’ point on a compact Grassmann manifold, $\mathbb{G}_M(\mathbb{C}^T)$, [3]. These basis vectors are rotated (and scaled) when right multiplied by the channel matrix \mathbf{H} , but since the receiver has no channel information, the rotation of the basis vectors cannot be detected. However, the subspace spanned by \mathbf{Q}_X is detectable [3]. In fact, the likelihood of the received signal given a transmitted unitary matrix satisfies [1], [3]

$$\begin{aligned} & P(\mathbf{Y}|\mathbf{Q}_X) \\ & \propto \exp\left(-\frac{\rho T}{M} \text{Tr}\left(\mathbf{Y}^\dagger \left(\mathbf{I}_T - \frac{1}{1 + M/(\rho T)} \mathbf{Q}_X \mathbf{Q}_X^\dagger\right) \mathbf{Y}\right)\right). \end{aligned} \quad (2)$$

In Figure 1 we show how the generic structure of a BICM-IDD scheme (e.g., [5]) can be adapted to the case of non-coherent MIMO communication. The outer components consist of a standard binary encoder and its corresponding soft-input/soft-output decoder. The proposed design of the inner components, namely the constellation and mapper at the transmitter and the demapper at the receiver, is discussed in the following sections.

III. CONSTELLATION DESIGN AND LABELLING

Finding $T \times M$ unitary matrices that span isotropically distributed linear subspaces has been identified in [3] with the packing of spheres on the compact Grassmann manifold, $\mathbb{G}_M(\mathbb{C}^T)$; i.e., given a target cardinality $|\mathcal{C}|$, we seek a constellation \mathcal{C} with maximized minimum distance [14],

$$\{\mathbf{Q}_{X_i}\}_{i=1}^{|\mathcal{C}|} = \arg \max_{\{\mathbf{Q}_r: \mathbf{Q}_r^\dagger \mathbf{Q}_r = \mathbf{I}_M, r=1, \dots, |\mathcal{C}|\}} \min_{j \neq k} d(\mathbf{Q}_j, \mathbf{Q}_k), \quad (3)$$

where $d(\cdot, \cdot)$ is a distance metric on the Grassmann manifold. While several metrics have been considered (e.g., [2], [14]), it has been shown [15], [16] that the chordal Frobenius norm quantifies the perturbation due to noise in the received signal subspace, and hence that it conforms to the non-coherent MIMO communication model.

¹In this model, the channel remains constant for a block of T channel uses, and in each block the channel coefficients are statistically independent of those in other blocks; e.g., [3].

Several techniques for generating ‘‘good’’ constellations have been proposed. Some are based on algebraic constructions (e.g., [17], [18]), but their inherent structure typically inhibits the full exploitation of the underlying degrees of freedom. Other techniques are based on various optimization techniques for finding ‘‘good’’ solutions to (3); e.g., [14], [16]. Although these optimized constellations tend to perform better than the algebraic ones, their lack of structure makes their storage, regeneration and labelling quite unwieldy.

In our BICM transmission scheme we will use constellations designed via the two-phase rotation-based technique in [16], [19], as those constellations possess structure, but are better able to exploit the underlying degrees of freedom. In this technique a small proto-constellation, \mathcal{C}_p , is designed using an efficient numerical optimization technique. The final constellation is then expressed as the disjoint union of R rotated versions of the proto-constellation; that is,

$$\mathcal{C} = \coprod_{r=1}^R (\mathbf{I}_{|\mathcal{C}_p|} \otimes \Phi_r) \mathcal{C}_p, \quad (4)$$

where the constellations \mathcal{C}_p and \mathcal{C} are represented by one and R block diagonal matrices, respectively, \otimes denotes the Kronecker product, and $\{\Phi_r\}_{r=1}^R$ are $T \times T$ unitary matrices. An optimized set of matrices $\{\Phi_r\}_{r=1}^R$ can be obtained by using efficient optimization techniques on the group of unitary matrices, and the resulting constellations possess several desirable distance properties [16], [19].

In addition to the distance properties of the underlying constellation, the performance of a BICM-IDD scheme is also dependent on the labelling of the constellation points. However, labelling points in a Grassmannian constellation is difficult, because even for small dimensions, ‘‘good’’ constellations are not known to possess a structure that could be exploited to determine an appropriate labelling strategy. In practice, the number of (real) dimensions, $2M(T - M)$, can be quite large. Furthermore, numerical optimization of the mapping of large constellations (e.g., [8]) is a formidable task. In the case of rotation-based Grassmannian constellations, these difficulties can be mitigated by exploiting the inherent structure. This structure admits a labelling technique that mimics the principles of the set-partitioning technique, which, roughly speaking, assigns labels with small Hamming distances to points that lie at large distances in the signalling space. In particular, if the proto-constellation, \mathcal{C}_p , is properly designed, its points will lie at maximum distance in the signalling space. Since rotation preserves the distance between points in the proto-constellation [16], [19], the smaller distances in the final constellation, \mathcal{C} , occur between points that belong to different rotations of \mathcal{C}_p . Using this insight, we now describe our labelling strategy.

Consider a rotation-based constellation with $|\mathcal{C}_p| = 2^{n_1}$ and $R = 2^{n_2}$. The mapper $\mathcal{M}(\cdot)$ is required to label the points of the constellation with binary vectors of length $n = n_1 + n_2$. We will use the first n_1 bits to index the point on the underlying proto-constellation and the remaining bits to index the rotation. By partitioning the label in this way, we ensure that constellation points generated by the same rotation, which will be well-spaced (so long as the proto-constellation is

well-designed), differ by a Hamming distance of at most n_1 . The remaining n_2 bits label the rotation, and since there is no known structure for these rotations, they will be chosen pseudo-randomly. By partitioning the labels in this way, we highlight the fact that the choice of the cardinality of the proto-constellation and the number of rotations provides a trade-off between favourable geometric and Hamming distance properties of transmitted codewords.

IV. NON-COHERENT SOFT DEMAPPING

The role of the (soft) demapper in a BICM-IDD scheme is to compute (or approximate) the (conditioned) log likelihood ratio (LLR) of each (encoded interleaved) bit given the received signal matrix. If we let x_k denote the k^{th} element of the length- n block of \mathbf{x} in Figure 1 associated with a given channel use, and if we let \mathbf{Y} denote the corresponding received matrix, then the LLR is (e.g., [5])

$$\begin{aligned} L_{D_1}(x_k|\mathbf{Y}) &= \ln \frac{P(x_k = +1|\mathbf{Y})}{P(x_k = -1|\mathbf{Y})} \\ &= \ln \frac{\sum_{\mathbf{Q}_X \in \mathcal{X}_{k,+1}} P(\mathbf{Y}|\mathbf{Q}_X)P(\mathbf{Q}_X)}{\sum_{\mathbf{Q}_X \in \mathcal{X}_{k,-1}} P(\mathbf{Y}|\mathbf{Q}_X)P(\mathbf{Q}_X)}, \quad (5) \end{aligned}$$

where an expression for $P(\mathbf{Y}|\mathbf{Q}_X)$ was given in (2), and an approximation to $P(\mathbf{Q}_X)$ can be obtained from the decoder outputs at the previous iteration using the standard assumption of independence of the interleaved encoded bits (e.g., [5]); i.e., $P(\mathbf{Q}_X) \approx \prod_{k=1}^n P(x_k = [\mathcal{M}^{-1}(\mathbf{Q}_X)]_k)$, where $[\cdot]_k$ denotes the k^{th} element of the vector. The set $\mathcal{X}_{k,+1}$ contains all the matrices \mathbf{Q}_X in the constellation whose indices have $x_k = +1$; i.e., $\mathcal{X}_{k,\pm 1} = \{\mathbf{Q}_X \in \mathcal{C} | x_k = [\mathcal{M}^{-1}(\mathbf{Q}_X)]_k = \pm 1\}$.

For most MIMO BICM schemes, the computation of the LLRs in (5) is the computational bottleneck. List-based demappers reduce this bottleneck by approximating the LLRs by computing the summations over a subset of the constellation points, \mathcal{L} , rather than over the whole constellation; i.e., $\mathcal{X}_{k,\pm 1}$ is replaced by $\tilde{\mathcal{X}}_{k,\pm 1} = \{\mathbf{Q}_X \in \mathcal{L} | x_k = [\mathcal{M}^{-1}(\mathbf{Q}_X)]_k = \pm 1\}$. In coherent MIMO systems the inherent tree structure of the demapping problem can be exploited in the construction of the list (e.g., [5]), but the geometry of the non-coherent case is substantially different, and an alternative approach is required. We propose to choose the demapping list \mathcal{L} to be the list generated by the reduced-search non-coherent detector for the uncoded Grassmannian constellations developed in [15], [16], [20]. That list is briefly described in Section IV-A.

A. List-based Demapper

The reduced-search detector developed in [15], [16], [20] uses the structure of Grassmannian constellations and the received signal \mathbf{Y} to determine a list of candidate constellation points. The generation of the list is based on the QR decomposition, $\mathbf{Y} = \mathbf{Q}_Y \mathbf{R}_Y$, and the observation [16], [20] that all the information available about \mathbf{Q}_X is contained in \mathbf{Q}_Y , while all that about \mathbf{H} is contained in \mathbf{R}_Y . The list is generated as follows: Prior to operation, the demapper picks a reference point $\mathbf{Q}_{\text{ref},1}$ and builds a look-up table in which the constellation points are sorted according to their distance

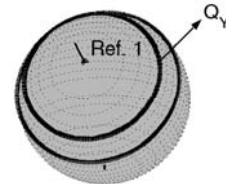


Fig. 2. A “strap” on the Grassmann manifold $\mathbb{G}_1(\mathbb{R}^3)$ that contains \mathbf{Q}_Y .

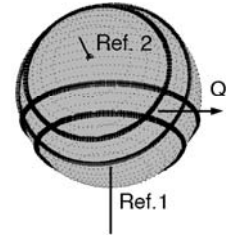


Fig. 3. The intersection of two “straps” on the Grassmannian manifold $\mathbb{G}_1(\mathbb{R}^3)$.

from the reference point. When a received signal matrix \mathbf{Y} arrives, its QR decomposition is computed and the distance $d(\mathbf{Q}_Y, \mathbf{Q}_{\text{ref},1})$ is measured. All constellation points that are “about the same distance” from the reference point as \mathbf{Q}_Y are included in the candidate list. More specifically, the channel information implicit in \mathbf{R}_Y is used to generate two values, A_Y and B_Y , which are used to define the width of a “strap” on the Grassmann manifold that contains \mathbf{Q}_Y ; see Figure 2 for an illustration and [16], [20] for the details. The demapper’s list is defined to be all those constellation points that lie within the strap; i.e.,

$$\begin{aligned} \mathcal{L}(\mathbf{Y}, \mathbf{Q}_{\text{ref},1}) \\ = \{\mathbf{Q}_X | A_Y \leq d(\mathbf{Q}_X, \mathbf{Q}_{\text{ref},1}) - d(\mathbf{Q}_Y, \mathbf{Q}_{\text{ref},1}) \leq B_Y\}. \quad (6) \end{aligned}$$

The choice of A_Y and B_Y involves a trade-off between the length of the list and the probability that the transmitted constellation point is not in the list. In particular, using the Chebychev inequality, one can find a lower bound on the width of the strap $|A_Y - B_Y|$ that is required for the probability of “missing” the transmitted constellation point to be below a given threshold [16], [20]. A feature of the proposed demapper is that the length of the list is adapted to the channel realization (through A_Y and B_Y). This is in contrast to the demapper for coherent MIMO systems proposed in [5], in which the length of the candidate list is fixed *a priori* and is made as large as possible subject to acceptable receiver complexity. In order to operate with an even shorter list, the look-up table in the proposed demapper can be augmented to include distances from other reference points, $\mathbf{Q}_{\text{ref},j}$. Each reference point can be used to generate a strap, and only those constellation points that lie in the intersection of the straps are assigned to the list; see Figure 3. That is, the list is $\mathcal{L} = \{\mathbf{Q}_X | \mathbf{Q}_X \in \bigcap_j \mathcal{L}(\mathbf{Y}, \mathbf{Q}_{\text{ref},j})\}$.

B. List Augmentation for the List-based Demapper

A weakness of the above list-based (soft) demapping scheme is that membership of the list is determined entirely

by the channel output, and hence a constellation point whose binary index is deemed by the decoder to have a large likelihood might not be on the demapper's list. To mitigate this effect, we will modify the list-based demapper to enable the decoder to augment the list of candidate constellation points. In particular, using Figure 1, let $L_{A_1}^{[i]}$ denote the vector of *a priori* information used by the demapper in the i^{th} iteration. Before performing the list-based demapping for a given channel use at the i^{th} iteration, the demapper makes an (auxiliary) hard decision on the corresponding length- n block of $L_{A_1}^{[i]}$ and checks whether the constellation point that corresponds to that hard decision is on the demapper's current list. If not already on the list, this constellation point is added; i.e.,

$$\mathcal{L}^{[i]} = \mathcal{L}^{[i-1]} \cup \left\{ \mathcal{M} \left(\text{sgn} \left((L_{A_1}^{[i]}(x_k))_{k=1}^n \right) \right) \right\}, \quad (7)$$

and the list-based demapper approximates the LLRs by computing (5) with the ranges of the summations being $\tilde{\mathcal{X}}_{k,\pm 1}^{[i]} = \{ \mathbf{Q}_X \in \mathcal{L}^{[i]} | x_k = [\mathcal{M}^{-1}(\mathbf{Q}_X)]_k = \pm 1 \}$. Since we add at most one constellation point to the demapper's list at each iteration, the increase in complexity is typically negligible. While more elaborate list augmentation strategies can be conceived, in the example in Figure 4 our simple augmentation scheme appears to extract much of the potential gain.

V. SIMULATION RESULTS

We consider a system with $M = N = 2$ and a coherence time $T = 4$. The outer codes in Figure 1 were chosen to be systematic parallel concatenated turbo codes with identical recursive convolutional constituent codes, and the BICM and "turbo" interleavers were selected from sets of pseudo-randomly generated candidates. At the receiver, four demapping-decoding iterations were performed for each block, with eight BCJR-based "turbo" iterations being performed within the outer decoder for each demapping-decoding iteration. In the list-based demapping schemes, the LLRs were clipped at ± 10 . Since no convenient expression is available for the ergodic capacity of a non-coherent MIMO block-fading channel, the high-SNR capacity approximation derived in [3] is used to provide an approximate SNR threshold for the rates considered in each of the following examples. These approximate thresholds are given in the caption of the respective figures.

In order to illustrate the impact of the list augmentation procedure in Section IV-B, in Figure 4 we have plotted the performance of our Grassmannian BICM-IDD scheme using full demapping and using the proposed list-based demapping technique, with and without list augmentation. For this experiment we used a 256-point Grassmannian constellation with a randomly chosen mapping and a standard rate-1/2 punctured turbo code with constituent codes of memory 4 and an input block length 8000. The resulting overall data rate was 1 bit per channel use (bpcu). Figure 4 shows that in the absence of list augmentation the performance of the list-demapper degrades with increasing SNR. For instance, at a BER of 10^{-4} the SNR gap to the full demapper is about 1.75 dB. By incorporating list augmentation, this gap is reduced to less than 0.25 dB. In Figure 4 we have also plotted the performance of a BICM

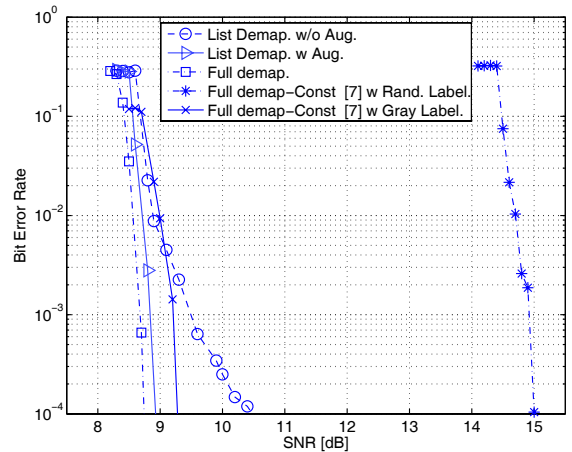


Fig. 4. Bit error rate performance of the proposed Grassmannian BICM-IDD scheme using full demapping (dash-dot), and using list-based demapping with (solid) and without (dashed) list augmentation. A comparison with a scheme that uses the constellation proposed in [7] and full demapping is also provided. The approximate SNR threshold for a rate of 1 bpcu is about 7.3 dB.

scheme that uses the orthogonal design proposed in [7] with full demapping. It can be seen that the stringent algebraic structure of those constellations results in an SNR gap of about 6.2 dB with respect to our constellations when random mapping is employed. Figure 4 also shows that by using the Gray labelling technique provided in [9], the performance gap between the scheme based on the orthogonal design and that based on our randomly mapped constellation can be reduced to 0.5 dB. We believe that the remaining gap is due to the difference between the distance properties of our constellation and those of the orthogonal design.

In Figure 5 we compare the performance of our proposed scheme with several training-based schemes. (Comparisons with training-based schemes at low data rates are available in [21].) For these simulations, the outer code was a rate-4/5 punctured turbo code with input block length 32,016. Using the notation in [22], the partition of each constituent convolutional code was $(2, 1, 1, 1)$, and its octal generators were $z^{\{1i\}} = (6, 0, 2, 3)$, $h^{\{1i\}} = (0, 6, 0, 5)$, $h^{\{2i\}} = (0, 3, 0, 1)$, $h^{\{3i\}} = (1, 2, 0, 3)$, and $h^{\{4i\}} = (2, 3, 3, 2)$. For the proposed scheme, a 4096-point Grassmannian constellation was generated using the rotation-based technique described in Section III and the associated quasi-set-partitioning labelling, yielding an overall data rate of 2.4 bpcu.

In the training-based schemes, the coherence time, T , was split into a training interval of length $T_p = M = 2$ and a coherent communication interval of length $T_d = T - T_p = 2$, with transmitted symbols \mathbf{X}_p and \mathbf{X}_d , respectively. (Choosing $T_p = M$ is optimal at high SNRs [10].) We employed the optimal training symbol $\mathbf{X}_p \propto \mathbf{I}_M$, [10], and since $T_d = M$ we allocated power equally to the training and data phases [10]. The scalar constellations used to construct \mathbf{X}_d were chosen so that the overall data rate was 2.4 bpcu. For comparison with our quasi-set-partitioning labelling technique, these constellations were labelled using full set-partitioning. Two demappers were considered for each of the training-based schemes. The "mismatched" demapper (e.g., [13]) uses

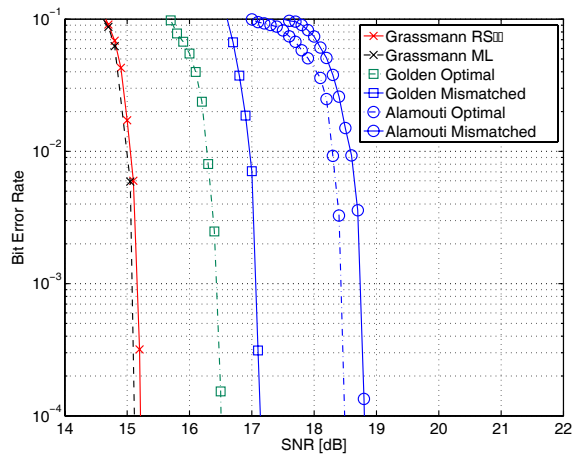


Fig. 5. Bit error rate performance of the proposed Grassmannian BICM-IDD scheme with full and list-based demapping, and that of several training-based BICM-IDD schemes with full demapping using “mismatched” and “optimal” demapping metrics. The approximate SNR threshold for a rate of 2.4 bpcu is about 11.7 dB.

\mathbf{X}_p and \mathbf{Y}_p to generate an estimate of the channel matrix, $\hat{\mathbf{H}}$, and then uses $\hat{\mathbf{H}}$ to perform coherent demapping as if it were the actual channel matrix. That is, the mismatched demapper computes the LLRs using a formula akin to (5), but with $P(\mathbf{Y}|\mathbf{Q}_X)$ replaced by $\exp(-\frac{\rho^T}{M}\|\mathbf{Y}_d - \mathbf{X}_d\hat{\mathbf{H}}\|_F^2)$, where $\|\cdot\|_F$ is the Frobenius norm. While this demapper has a simple structure, better performance can be achieved using a receiver that uses the “optimal” demapping metric (e.g., [13]), which does not involve explicit estimation of the channel; that is, by using $P(\mathbf{Y}_p, \mathbf{Y}_d|\mathbf{X}_p, \mathbf{X}_d)$ in place of $\exp(-\frac{\rho^T}{M}\|\mathbf{Y}_d - \mathbf{X}_d\hat{\mathbf{H}}\|_F^2)$.

In Figure 5 we compare the performance of the proposed Grassmannian-signalling scheme using both full and list demapping (with augmentation), with that of several training-based schemes that use mismatched or optimal demapping, with full lists. (In all systems the outer encoder and decoder are the same.) In the first training-based scheme the data matrices were generated using the Alamouti scheme [23] with 64-QAM symbols. If the “mismatched” demapper is used, our proposed scheme has an SNR advantage of about 3.75 dB over this training-based scheme, and even if the “optimal” demapper is used, the gap remains about 3.3 dB. A more sophisticated training-based scheme can be constructed using the Golden code [24], with scalar symbols drawn from a rectangular 8-QAM constellation (so that the overall data rate is 2.4 bpcu). The performance of the resulting scheme with both mismatched and optimal demapping is also plotted in Figure 5. Although the use of the “optimal” demapper provides a considerable performance gain over the mismatched receiver for the Golden code scheme, the proposed Grassmannian signalling scheme provides even better performance. In particular, our scheme has an SNR advantage of about 2 dB and 1.4 dB over the Golden code schemes with mismatched and

optimal demapping, respectively.² An additional advantage of the proposed approach is that it can be adapted to different antenna configurations and target rates in a straightforward way. This is not always the case with sophisticated coherent codes.

VI. CONCLUSION

We have developed a BICM-IDD scheme for a Grassmannian signalling approach to non-coherent MIMO communication, and we have demonstrated that for high data rate transmission over channels with short coherence times, the proposed scheme can provide significantly better performance than several training-based schemes.

REFERENCES

- [1] T. L. Marzetta and B. M. Hochwald, “Capacity of a mobile multiple-antenna communication link in Rayleigh flat fading,” *IEEE Trans. Inform. Theory*, vol. 45, pp. 139-157, Jan. 1999.
- [2] B. M. Hochwald and T. L. Marzetta, “Unitary space-time modulation multiple-antenna communications in Rayleigh flat fading,” *IEEE Trans. Inform. Theory*, vol. 46, pp. 543-564, Mar. 2000.
- [3] L. Zheng and D. Tse, “Communication on the Grassmann manifold: a geometric approach to the noncoherent multiple-antenna channel,” *IEEE Trans. Inform. Theory*, vol. 48, pp. 359-383, Feb. 2002.
- [4] G. Caire, G. Taricco, and E. Biglieri, “Bit-interleaved coded modulation,” *IEEE Trans. Inform. Theory*, vol. 44, pp. 927-945, May 1998.
- [5] B. M. Hochwald and S. ten Brink, “Achieving near-capacity on a multiple-antenna channel,” *IEEE Trans. Commun.*, vol. 51, pp. 389-399, Mar. 2003.
- [6] I. Bahceci and T. M. Duman, “Combined turbo coding and unitary space-time modulation,” *IEEE Trans. Commun.*, vol. 50, pp. 1244-1249, Aug. 2002.
- [7] W. Zhao, G. Leus, and G. B. Giannakis, “Orthogonal design of unitary constellations for uncoded and trellis-coded noncoherent space-time systems,” *IEEE Trans. Inform. Theory*, vol. 50, pp. 1319-1327, June 2004.
- [8] Y. Li and X. G. Xia, “Constellation mapping for space-time matrix modulation with iterative demodulation/decoding,” *IEEE Trans. Commun.*, vol. 53, pp. 764-768, May 2005.
- [9] N. H. Tran, H. H. Nguyen, and T. Le-Ngoc, “Coded unitary space-time modulation with iterative decoding: error performance and mapping design,” *IEEE Trans. Commun.*, vol. 55, pp. 703-716, Apr. 2007.
- [10] B. Hassibi and B. Hochwald, “How much training is needed in multiple-antenna wireless links?” *IEEE Trans. Inform. Theory*, vol. 49, pp. 951-963, Apr. 2003.
- [11] P. Dayal, M. Brehler, and M. K. Varanasi, “Leveraging coherent space-time codes for noncoherent communication via training,” *IEEE Trans. Inform. Theory*, vol. 50, pp. 2058-2080, Sept. 2004.
- [12] H. El Gamal, D. Aktas, and M. O. Damen, “Noncoherent space-time coding: an algebraic perspective,” *IEEE Trans. Inform. Theory*, vol. 51, pp. 2380-2390, July 2005.
- [13] G. Taricco and E. Biglieri, “Space-time decoding with imperfect channel estimation,” *IEEE Trans. Wireless Commun.*, vol. 4, pp. 1874-1888, July 2005.
- [14] D. Agrawal, T. Richardson, and R. Urbanke, “Multiple-antenna signal constellations for fading channels,” *IEEE Trans. Inform. Theory*, vol. 47, pp. 2618-2626, Sept. 2001.
- [15] R. H. Gohary and T. N. Davidson, “Non-coherent MIMO communication: Grassmannian constellations and efficient detection,” in *Proc. IEEE Int. Symp. Inform. Theory*, Chicago, USA, June 2004.
- [16] R. H. Gohary and T. N. Davidson, “Non-coherent MIMO communication: Grassmannian constellations and efficient detection,” to appear in *IEEE Trans. Inform. Theory*.

²Although the optimal demapper provides improved performance, it is not immediately obvious that a corresponding list-based demapper can be constructed. Furthermore, computing each $\ln P(\mathbf{Y}_p, \mathbf{Y}_d|\mathbf{X}_p, \mathbf{X}_d)$ requires $O(TNM) + O(NM^2)$ operations, whereas computing the corresponding term in the mismatched and non-coherent demappers requires $O(T_dNM)$ and $O(NT^2)$ operations, respectively. (These expressions neglect the terms that can be pre-computed and the cost of any channel estimation.)

- [17] V. Tarokh and I.-M. Kim, "Existence and construction of noncoherent unitary space-time codes," *IEEE Trans. Inform. Theory*, vol. 48, pp. 3112-3117, Dec. 2002.
- [18] B. M. Hochwald, T. L. Marzetta, T. J. Richardson, W. Sweldens, and R. Urbanke, "Systematic design of unitary space-time constellations," *IEEE Trans. Inform. Theory*, vol. 46, pp. 1962-1973, Sept. 2000.
- [19] R. H. Gohary and T. N. Davidson, "On the design of Grassmannian constellations for non-coherent MIMO communication systems," in *Proc. IEEE Canad. Wkshp Inform. Theory*, Edmonton, Canada, pp. 114-117, June 2007.
- [20] R. H. Gohary and T. N. Davidson, "On efficient non-coherent detection of Grassmannian constellations," in *Proc. IEEE Int. Symp. Inform. Theory*, Adelaide, Australia, pp. 1676-1680, Sept. 2005.
- [21] M. A. El-Azizy, R. H. Gohary, and T. N. Davidson, "A BICM scheme with iterative demapping and decoding for non-coherent MIMO communication," in *Proc. IEEE Int. Conf. Commun.*, Istanbul, Turkey, pp. 4107-4112, June 2006.
- [22] S. Benedetto, R. Garello, and G. Montorsi, "A search for good convolutional codes to be used in the construction of turbo codes," *IEEE Trans. Commun.*, vol. 46, pp. 1101-1105, Sept. 1998.
- [23] S. M. Alamouti, "A simple transmitter diversity scheme for wireless communications," *IEEE J. Select. Areas Commun.*, vol. 16, pp. 1451-1458, Oct. 1998.
- [24] J.-C. Belfiore, G. Rekaya, and E. Viterbo, "The Golden code: a 2×2 full-rate space-time code with nonvanishing determinants," *IEEE Trans. Inform. Theory*, vol. 4, pp. 1432-1436, Apr. 2005.